Available online at www.sciencedirect.com
SCIENCE DIRECT
Journal of Power Sources 156 (2006) 267–280
JOURNAL OF POWER SOURCES
www.elsevier.com/locate/jpowsour

Water flooding and two-phase flow in cathode channels of proton exchange membrane fuel cells

Xuan Liu [a,b], Hang Guo [a,b,*], Chongfang Ma [a,b]

[a] *Key Laboratory of Enhanced Heat Transfer and Energy Conservation, Ministry of Education of China, College of Environmental and Energy Engineering, Beijing University of Technology, No. 100 Pingleyuan, Chaoyang District, Beijing 100022, PR China*

[b] *Beijing Municipal Key Laboratory of Heat Transfer and Energy Conversion, College of Environmental and Energy Engineering, Beijing University of Technology, Beijing 100022, PR China*

Received 16 April 2005; received in revised form 9 June 2005; accepted 10 June 2005
Available online 18 August 2005

Abstract

The water flooding and two-phase flow of reactants and products in cathode flow channels (0.8 mm in width, 1.0 mm in depth) were studied by means of transparent proton exchange membrane fuel cells. Three transparent proton exchange membrane fuel cells with different flow fields including parallel flow field, interdigitated flow field and cascade flow field were used. The effects of flow field, cell temperature, cathode gas flow rate and operation time on water build-up and cell performance were studied, respectively. Experimental results indicate that the liquid water columns accumulating in the cathode flow channels can reduce the effective electrochemical reaction area; it makes mass transfer limitation resulting in the cell performance loss. The water in flow channels at high temperature is much less than that at low temperature. When the water flooding appears, increasing cathode flow rate can remove excess water and lead to good cell performance. The water and gas transfer can be enhanced and the water removal is easier in the interdigitated channels and cascade channels than in the parallel channels. The cell performances of the fuel cells that installed interdigitated flow field or cascade flow field are better than that installed with parallel flow field. The images of liquid water in the cathode channels at different operating time were recorded. The evolution of liquid water removing out of channels was also recorded by high-speed video.

Keywords: Proton exchange membrane fuel cell; Visualization; Flow field; Two-phase flow; Flooding

1. Introduction

Proton exchange membrane fuel cells (PEMFCs) have reached the stage of being in the forefront among the different types of fuel cells. PEMFCs have many advantages such as using solid polymer electrolytes, low operating temperatures, cold start-up, high-energy efficiency and power density [1–3]. PEMFCs not only have been used for space, military, distributed power stations, but also were developed for electric vehicles and mobile devices [4,5].

More and more researchers have recognized that there are many thermophysical issues in the fields of PEMFCs [6]. Problems of mass transfer in PEMFCs are key issue to the cell performance. They include: (i) water flooding: liquid water entrapped inside the electrodes or flow channels interrupts the flux of reactant/product gases; (ii) depletion of gas: the oxidant and fuel transport along the flow channels and penetrate through gas diffusion layer to electrochemical sites [7]. Concentration polarization occurs when the chemical reaction is limited by the rate at which reactants can be supplied. In the region of concentration polarization, losses due to mass transport limitations are dominant. This lack of reactants slows down the electrochemical reaction, resulting in a lower cell potential.

* Corresponding author. Tel.: +86 10 67391985x8311; fax: +86 10 67392774.
E-mail address: hangguo@sohu.com (H. Guo).

0378-7753/$ – see front matter © 2005 Elsevier B.V. All rights reserved.
doi:10.1016/j.jpowsour.2005.06.027

Water and thermal management is essential for the proper operation of PEMFCs [8]. The polymer membrane in the PEMFCs must be in a hydrated state to facilitate proton transport. If there is not enough water, the membrane becomes dehydrated and its resistance to proton conduction increases sharply. On the other hand, if too much water is present, flooding may occur, and the pores of the gas diffuser may be filled by liquid water, which will block the transport of reactants to the reaction sites. Indeed, water flooding often acts as the main cause of serious performance drop at high current densities [9].

In PEMFCs, the water distribution in the membrane is determined by two main mechanisms: electro-osmotic drag and diffusion [10]. Otherwise, the water is discharged electrochemically in the cathode. In practice, there is much more water resulting in flooding in the cathode than in the anode, especially at high current density and low temperature conditions. If the generated water is not removed from the electrode and flow channels at a sufficient rate, flooding appears and the transport of reactants is hindered [11]. Studies on the water transfer and water management have been widely published. Several modeling studies have been published in order to predict PEMFCs performance at given flooding levels [9,12–15]. During fuel cell operation, water may be supplied by humidified reactants or by direct liquid hydration [11,16–20]. Some new methods of preparing self-humidifying polymer electrolyte membranes, in which the catalysts were embedded, can also hydrate the polymer electrolyte membrane by the water generated from the electrochemical reactions [21–24]. But those studies did not present the images and patterns of liquid water in PEMFCs. In order to enhance the cell performance, the visualization of water distribution and multi-phase flow in the flow channels must be studied, which can help for optimizing operating conditions and flow field design to avoid flooding in PEMFCs.

Lu et al. [25] presented the visualization of bubble flow in the anode and water flooding in the cathode of a 5 cm^2 transparent DMFC with the flow field consisted of eight parallel flow channels (1.92 mm in width, 1.5 mm in depth). They studied the effects of backing pore structure and wettability on cell polarization characteristics and two-phase flow dynamics based on two different membrane electrode assemblies (MEAs). The water droplets, which appeared upon the gas diffusion layer (GDL) surface of the two different MEAs, were presented and the effect of the hydrophobicity of the GDL on the liquid droplets was examined. Tübe et al. [26] researched the visualization of liquid water in PEMFCs. A transparent PEMFC with two parallel air channels (1.5 mm in width, 1 mm in depth and 50 mm in length) was used in their studies. They only presented the images of the effect of operating time on water flooding and cell performance at a constant voltage operation mode, but discussed the effects of the air stoichiometry, temperature, air humidity and different characteristics of diffusion layers. The influence of hydrophobic and hydrophilic diffusion layers compared to standard carbon papers on water transport was investigated. Hackenjos et al. [27] designed a PEMFC for the combined measurement of current distribution at anode flow field and temperature distribution and flow field flooding at cathode flow field. The cathode flow field was a single channel meander with 1 mm channel width and 1 mm wide ribs in between. They showed the photos and investigated the relationship between the current and temperature distribution and flow field flooding at air flow rates of 250 sccm, 500 sccm and 750 sccm.

In this paper, the visualization of liquid water in three transparent PEMFCs with different types of cathode flow beds was shown. The water build-up and water flooding in multi-channels were studied experimentally. The effects of cell temperatures, cathode gas flow rates, and operating time on the water flooding and cell performance were examined. The water flooding and two-phase flow of reactants and products in cathode flow fields were recorded.

2. Experimental

2.1. Transparent PEMFCs

Membrane electrode assemblies made by Fuyuan Century Fuel Cell Power Co. Ltd. were used. The MEA was composed of Nafion 1135 membrane that was sandwiched between two carbon papers. Both the anode and the cathode were loaded with Platinum of 0.4 mg cm^{-2}. The active area was 5 cm^2.

In order to investigate the liquid water and water flooding inside PEMFCs, three transparent PEMFCs were used in our research. Fig. 1 shows the schematics of the cathode side of the three transparent PEMFCs and the diagrams of the gas flow passages. The stainless steel plate was used as the cathode flow field and current collector. Plexiglass was the transparent material outside the cathode flow field. The thickness of the stainless steel was 1 mm and there were nine slots of 0.8 mm width in it. Therefore, when the stainless steel was installed between the transparent plexiglass and MEA, the flow channels (0.8 mm in width, 1 mm in depth) were formed. A different designation of slots made the flow channels difference. In this study, we used three types of flow channels (shown in Fig. 1). Teflon coated glass fiber clothes with the matching slots were sandwiched between the flow field and the plexiglass as the sealing strip. Two main channels as the manifolds, flow in and flow out, in the transparent plexiglass connected the channels of the fuel cell flow field and the pipelines of the experimental system. In the anode side, graphite was used as the anode flow field material. Another two stainless steel plates were used for clamping. A window was set up in the cathode clamping plate so that we were able to unobstructively observe the water build-up and flooding inside the PEMFC. An electrical heating rod was inserted into the anode steel plate to heat the fuel cell. A unit temperature controller including electromagnetic relay and temperature sensor (PT100) was used to control the cell temperatures.

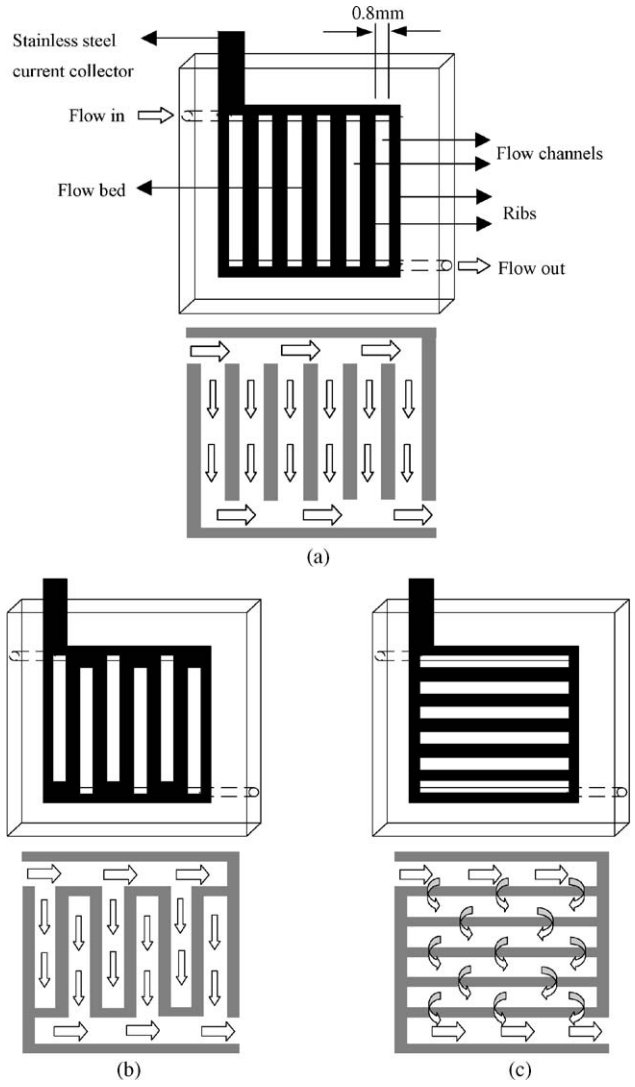

Fig. 1. Schematics and diagrams of the cathode side of transparent PEMFCs. (a) Parallel flow field, (b) interdigitated flow field and (c) cascade flow field.

2.2. Experimental set-up

Fig. 2 shows the experimental set-up. The experimental set-up consists of: (i) a fuel and oxidant reactant supply system; (ii) a cell performances test system; (iii) a high-speed video and digital camera recording system; (iv) a data collector and analysis system.

Pure hydrogen and oxygen were used as fuel and oxidant reactant, respectively. The gases to the fuel cells were not humidified; so all the water we observed in the flow channels of the transparent fuel cells was generated only from the electrochemical reaction. Gas flow rates were quantified by mass flow controllers (MFCs, Type SY 9312B-EX) with a precision of 0.5%. Gas pressures and pressure differences between the inlet and the outlet of the cathode were provided by pressure sensors (Type WQSBP) with a precision of 0.1% and pressure difference sensors (Type 1151DP) with a precision of 0.1%, respectively. A nitrogen purge system made sure to clean out the fuel and oxidant reactant left in the test system pipelines and fuel cells. An electronic load (Arbin FCTS LNR) was applied in the external circuit of the tested fuel cell. The flow patterns and images of water flooding in the cathode flow channels were recorded by the high-speed video (PHOTRON, FASTCAM 10K) and digital camera (Sony, DSC-F505V), respectively. The images in the video recorder were converted to computer pictures with the aid of a SCSI card and Readcam software.

3. Results and discussion

3.1. Water flooding in cathode channels

The water flooding in the transparent PEMFCs with three different types of flow channels are shown in Figs. 3–5. In this experiment, the oxygen flow rate was quantified at 30 ml min^{-1} and hydrogen flow rate was quantified at 50 ml min^{-1}. The fuel cells operated at a temperature of 25 °C and an ambient pressure. The photos were taken after the fuel cells had operated at a constant current of 2 A (0.4 A cm^{-2}) for 5 min. During operation, water droplets were appearing (condensing) in the cathode flow channels. The fact that water occurs near the outlet of the cathode channels is attributed to the resulting oxygen flow conditions. Because of the electrochemical reaction, the oxygen volume is decreasing along the channels. So at the end of the channels (outlet), the oxygen volume flow is much lower than that in the channels and the gas can hardly remove the condensation of liquid water. It shows that in PEMFCs, water produced by electrochemical reaction as waste can penetrate through the gas diffusion layer into the channels. When the water that is removed out of the channels is less than the water that is removed from the reaction sites, flooding may occur. As the result, cell performance decreases dramatically because the liquid phase boundary reduces the space of channels and occupies the path of the gas to the reaction sites. Generally, the effective area of electrochemical reaction is reduced and the mass transfer is limited because of the water columns.

It can be seen that the flooding appears downstream in the flow channels of the three flow fields, but the flooding patterns are different in different flow channels. In the parallel channels, all the liquid water accumulated and then formed water columns. But in the interdigitated channels, many water droplets condensed on the inner surface of the plexiglass and the water columns were much shorter than that in the parallel channels. In the cascade channels, the water columns also were found but the water was less than that in the parallel channels. There was also an obvious difference in the manifold (main channel). There was a lot of water in the manifolds (main channels) of the interdigitated field and the cascade field, but the manifold (main channel) of the parallel field was water free. The water that came from the electrochemical reaction accumulated in the parallel channels but was removed out of the interdigitated channels and cascade channels. The water in the manifolds (main channels) of the

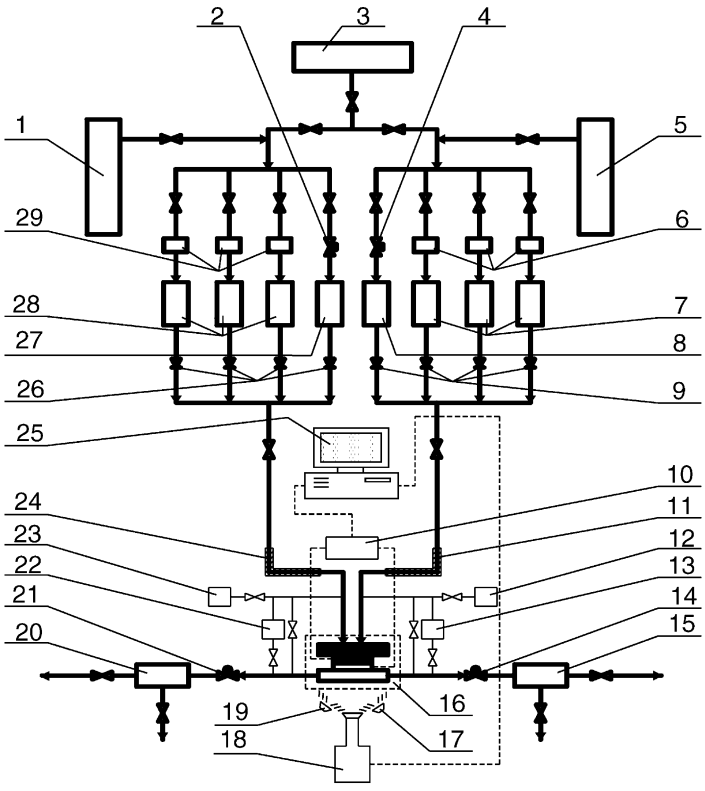

Fig. 2. Experimental set-up. (1) Hydrogen tank; (2) hydrogen regulator; (3) nitrogen tank; (4) oxygen regulator; (5) oxygen tank; (6) oxygen filter; (7) oxygen flow controller; (8) oxygen flowmeter; (9) oxygen one-way valve; (10) electronic load; (11) oxygen heating tape; (12) oxygen pressure transmitter; (13) oxygen pressure difference transmitter; (14) oxygen back pressure regulator; (15) oxygen condensing tank; (16) transparent fuel cell; (17 and 19) cold light source; (18) recording system; (20) hydrogen condensing tank; (21) hydrogen back pressure regulator; (22) hydrogen pressure transmitter; (23) hydrogen pressure difference transmitter; (24) hydrogen heat tape; (25) data recording system; (26) hydrogen one-way valve; (27) hydrogen flowmeter; (28) hydrogen flow controller; (29) hydrogen filter.

interdigitated field and the cascade field was the water that was removed by the cathode gas flow. The cathode gas flow is forced to go through the gas diffusion layer (Fig. 1) and reach the electrochemical reaction sites in the interdigitated channels and the cascade channels. When the gas goes through the gas diffusion layer, the water stays in the pores of the gas diffusion layer may be removed. So, the water and gas transfer can be enhanced in interdigitated channels and cascade channels, and the water removal is easier in interdigitated channels and cascade channels than in parallel channels. As the result, the cell performances of the fuel cells that installed interdigitated flow field and cascade flow field are better than that installed with parallel flow field (Fig. 6).

3.2. Effect of temperature

Whether the water is liquid or vapor in fuel cells flow channels depends on the temperature and pressure. At a constant

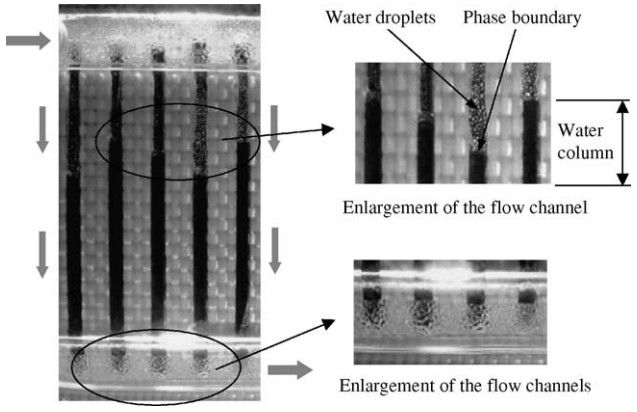

Fig. 3. Water flooding in parallel flow field.

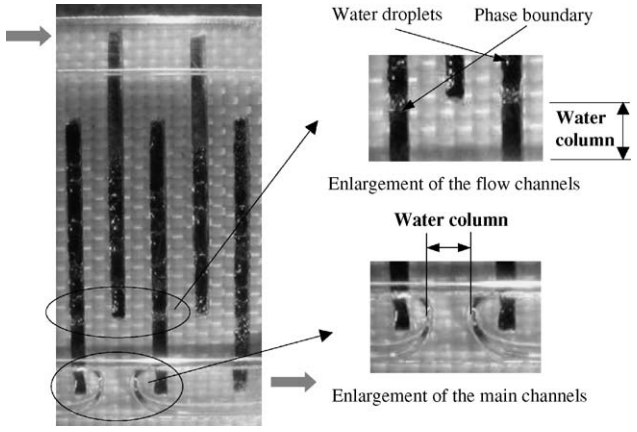

Fig. 4. Water flooding in interdigitated flow field.

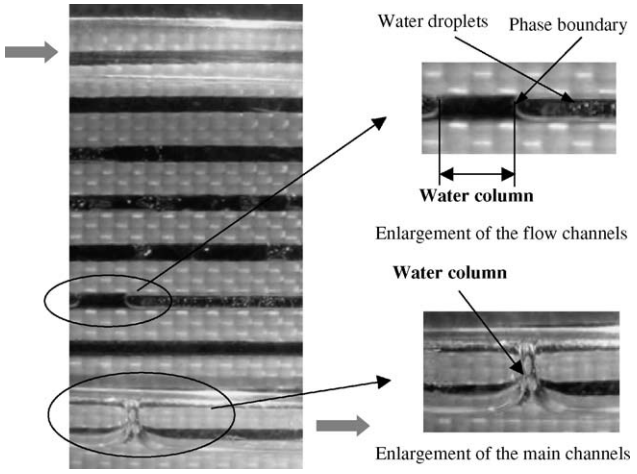

Fig. 5. Water flooding in cascade flow field.

pressure condition, a higher temperature can enhance vaporization. Vapor removal is easier than liquid water removal in such small flow channels because of the strong surface tension. Figs. 7–9 show the effect of cell temperature on the condensation of water in transparent PEMFCs. The fuel cells operated at the condition of atmosphere pressure, oxygen flow rate of 30 ml min^{-1} and hydrogen flow rate of 50 ml min^{-1}, and the constant current of 2 A (0.4 A cm^{-2}).

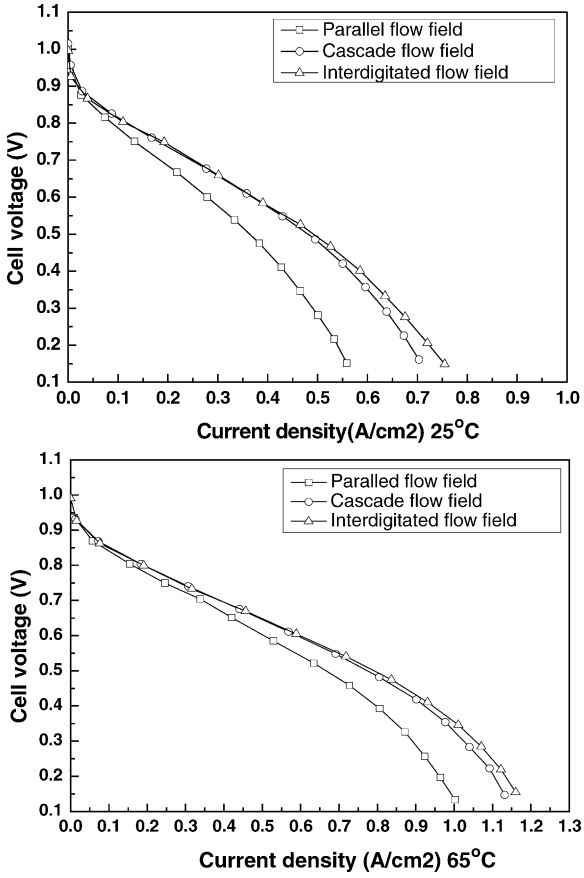

Fig. 6. Cell performances with different flow fields.

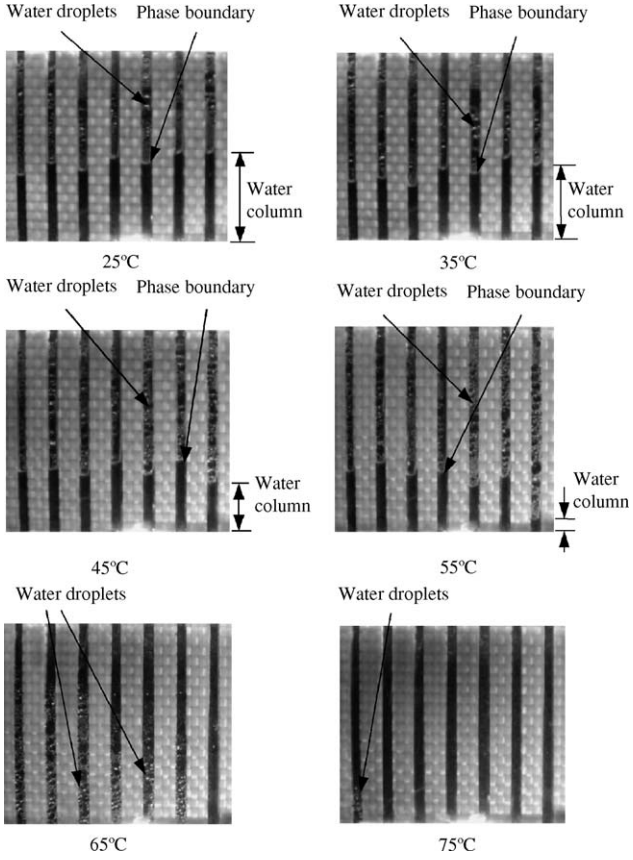

Fig. 7. Effect of cell temperature on cathode water build-up in parallel channels.

It is clear that the liquid water in flow channels at low temperature was much more than that at high temperature. When fuel cells operated at low temperatures, e.g. 25 °C, there was great volume of liquid water in the cathode flow channels. The water columns are the condensed water accumulating in the flow channels. The water columns not only can reduce the channels volume and effective electrochemical reaction areas, but also can obstruct mass transport. At this operating condition, the cell performance would be low because the flow channels were filled with the liquid water. With the increasing of the cell temperature, the water columns in the flow channels decreased because the vapor condensation rate at high temperature is much slower than that at low temperature. A lot of water vapor was removed out of the flow channels before condensation. So, at a higher temperature, e.g. 75 °C, the water columns disappeared and only a little liquid water with form of droplets was found in the flow channels.

The figures also show that at the same temperature condition, the images and patterns of water in the flow channels are different because of different flow fields. There were a lot of water droplets in the interdigitated channels and cascade channels but water columns in the parallel channels. The cathode gas flow passages are different (shown in Fig. 1) and their capacities for water removal are different. In the interdigitated channels and cascade channels, not enough water droplets

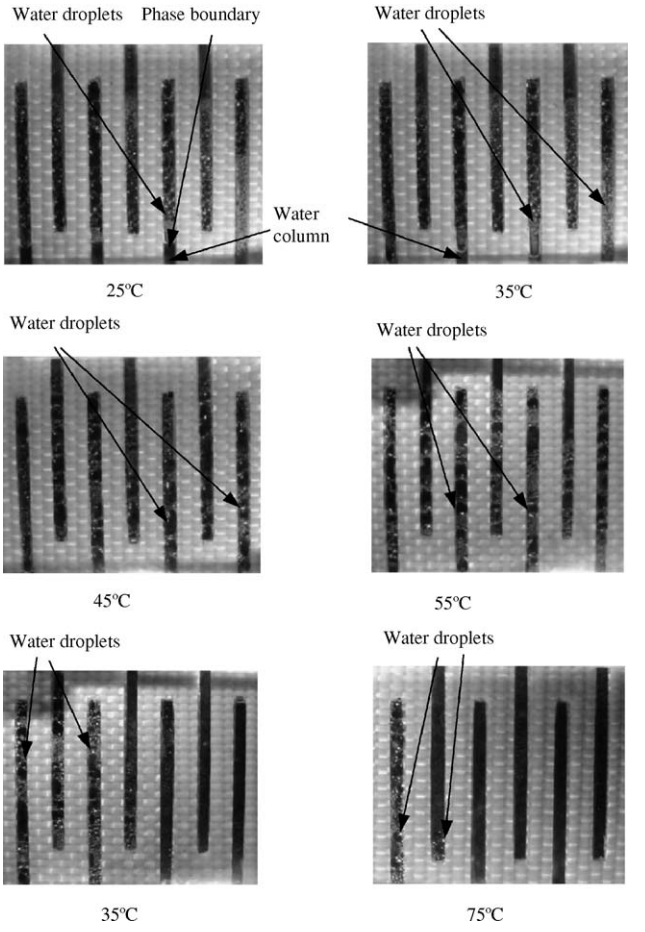

Fig. 8. Effect of cell temperature on cathode water build-up in interdigitated channels.

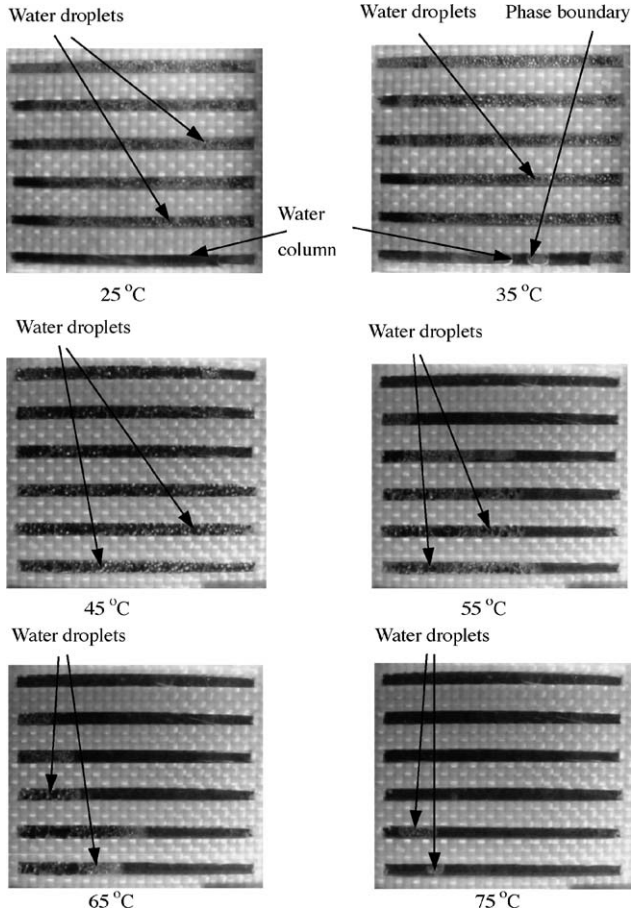

Fig. 9. Effect of cell temperature on cathode water build-up in cascade channels.

got together to form water columns. Enhancing mass transfer can help remove liquid water, so the accumulated water in the interdigitated channels and cascade channels was less than that in parallel channels at the same temperature.

In order to increase the activity of the catalyst, PEMFCs operate at temperatures of 70–80 °C. The cell temperature may affect the cell performance not only because it impacts on the activity of the catalyst but also because it is a key issue related to mass transfer. The photos display that at low temperature, too much condensation of liquid water in the flow channels hinders mass transfer because the water occupies the path of the reactant gas to the electrochemical sites. So, PEMFCs performance is low at low temperature due to the mass transfer limitation, which accompanies the low activation of the catalyst. By increasing the cell temperature, the condensation of liquid water in the cathode channels is decreased, and the mass transfer may be improved. But the cell temperature should not be too high. In Figs. 7–9, the condensation of liquid water was extremely little at the cell temperature of 75 °C. It is surmised that if the cell temperature had been elevated much higher, the water vapor could easily have been removed out of the flow channels without condensation, and there would not have been any liquid water in the fuel cells. But this is also a bad condition because there would not be enough water in the polymer membrane to facilitate proton transport. The membrane would become dry and its resistance to proton conduction will increase sharply and cell performance decrease dramatically. So PEMFCs must operate within a moderate temperature range. Otherwise, water management problems such as water flooding or membrane dehydration can happen, either of which can lead to cell performance drop. Therefore, water management is important to the fuel cell performance, which is related to the thermal management.

3.3. *Effect of oxygen flow rate*

The cathode gas flow rate can contribute to water removal. It has been reported in other papers that in PEMFCs, in order to reduce the concentration losses resulting from water flooding, the stoichiometric ratio must be at least 2 [9,28,29]. But if the cathode reactant is fully humidified, the stoichiometric ratio of the reactant has to be supplied at more than 43 to avoid liquid water [12]. Figs. 10–12 show the photos of condensation of liquid water in the cathode flow channels at different oxygen flow rates. These photos were taken at current of 2 A (0.4 A cm^{-2}) after the fuel cells had operated for 5 min at the air pressure and cell temperature of 25 °C. The oxy-

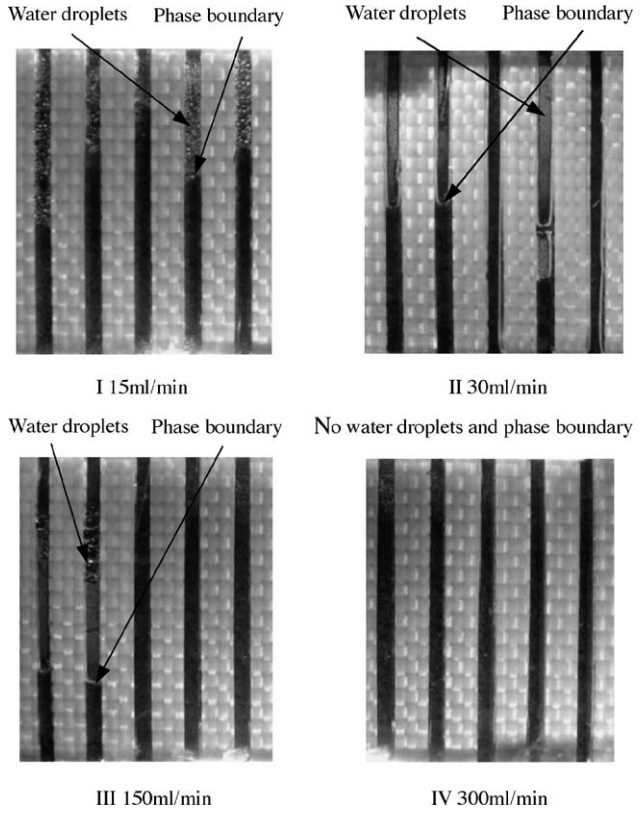

Fig. 10. Effect of oxygen flow rate on cathode water build-up in parallel channels.

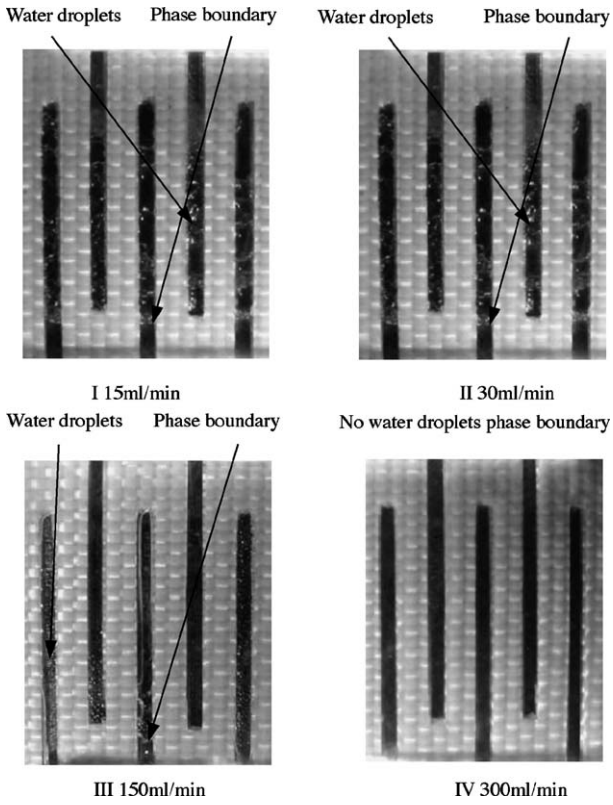

Fig. 11. Effect of oxygen flow rate on cathode water build-up in interdigitated channels.

gen flow rates were 15 ml min^{-1}, 30 ml min^{-1}, 150 ml min^{-1} and 300 ml min^{-1}, and accordingly, the stoichiometric ratios were 2.14, 4.29, 21.4 and 42.9, respectively. In those cases, the oxygen was not humidified. When the oxygen flow rate was less than 30 ml min^{-1}, it was too low to remove the water coming from the electrochemical sites of the fuel cells. Therefore, the water flooding in the flow channels was serious. So, during fuel cells operation, a sufficient cathode gas flow rate must be supplied to remove the excess liquid water out of the fuel cells. If the water removal with the oxygen is much less than that coming from the electrochemical sites, there will be flooding in the cathode flow channels.

The curves of cell voltage–operation time (Fig. 13) illustrate that the cell performance decreased continuously until the flow rate was increased. At every beginning of increasing the cathode gas flow rate, the cell performance increased sharply in a short time because of the sudden oxygen flow rate change. The curves also reveal that at the condition of oxygen flow rate less than 150 ml min^{-1}, increasing the oxygen flow rate can increase cell performance. When the oxygen flow rate was increased to 150 ml min^{-1}, the fuel cells operated at constant voltage. Fig. 13 implies that increasing the cathode gas flow rate can lead to good cell performance because high cathode gas flow rate can help the excess water removal out of the cathode flow channels and reduce the flooding. From the photos of 150 ml min^{-1} (Figs. 10–12), we can observe that most of liquid water was removed by the oxygen. When

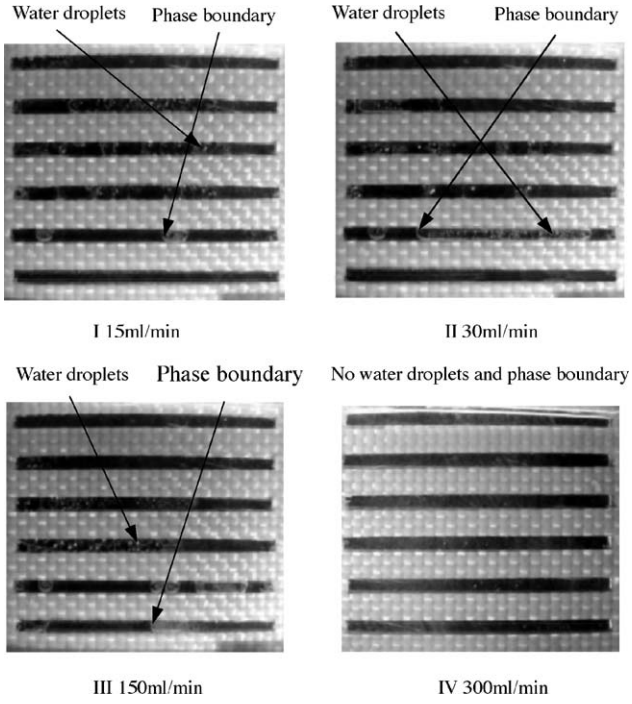

Fig. 12. Effect of oxygen flow rate on cathode water build-up in cascade channels.

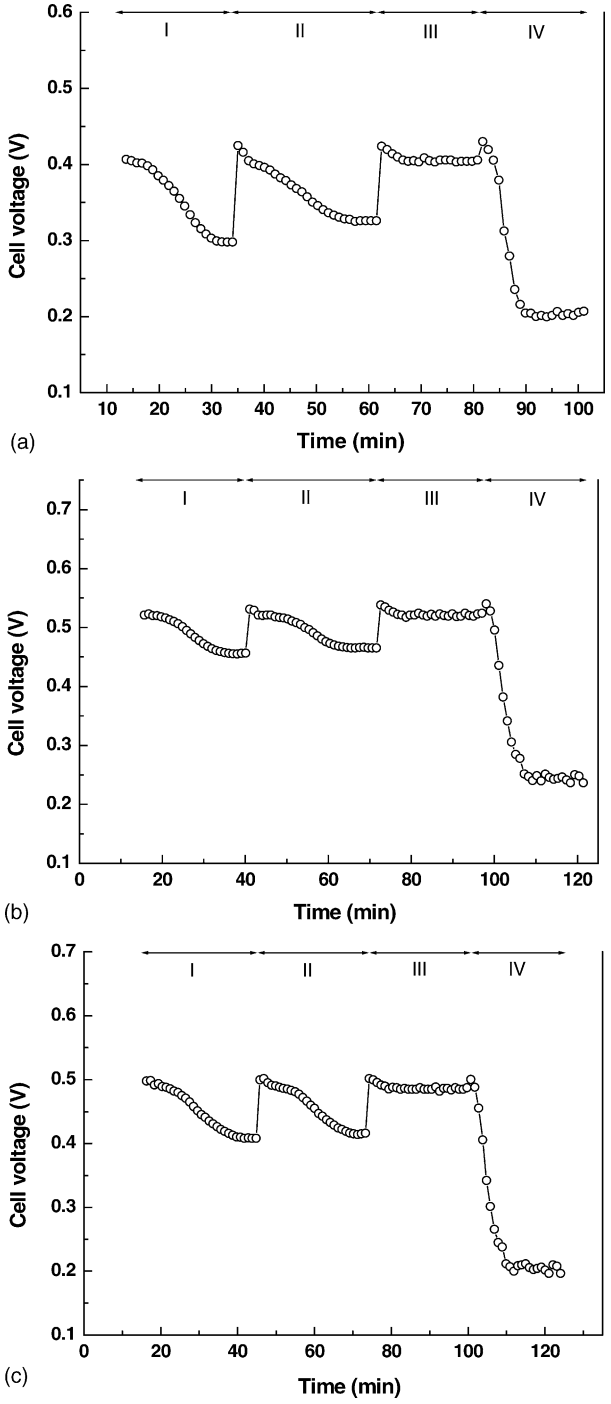

Fig. 13. Cell performance at different cathode flow rates with different flow channels. (a) Parallel flow channels; (b) interdigitated flow channels; (c) cascade flow channels.

the oxygen flow rate was increased to 300 ml min^{-1}, cell performance fell sharply because much higher oxygen flow rate removed too much water resulting in membrane dehydration. The results implied that in this condition, an oxygen flow rate of 150 ml min^{-1} was appropriate to operate fuel cells.

It was found that at the low cathode gas flow rate, less than 150 ml min^{-1}, the water columns in the parallel channels were much more than that in the interdigitated channels and cascade channels (Figs. 10–12). The flooding areas in interdigitated channels and cascade channels were much smaller than that in parallel channels. Because of enhanced mass transfer, interdigitated flow fields and cascade flow fields can remove more condensation of water than parallel flow fields even at low cathode gas flow rate. As the result, the cell performances of the fuel cells with interdigitated channels or cascade channels are better than those with parallel channels (Fig. 13).

The liquid water would not appear until the saturated vapor pressure of water $p_{sat}^{H_2O}$ is higher than the partial pressure of water in the oxygen $p_{O_2}^{H_2O}$ in this study. The maximum capacity of water removal by the oxygen flow out of the channels can be arrived when the saturated vapor pressure of water $p_{sat}^{H_2O}$ is equal to the partial pressure of water in the oxygen at the channels outlets $p_{O_2,\,out}^{H_2O}$.

$$p_{sat}^{H_2O} = p_{O_2,\,out}^{H_2O} \tag{1}$$

The saturated vapor pressure of water in bar can be expressed as a function of temperature (°C) [15]:

$$p_{sat}^{H_2O} = 10^{-2.174+2.953\times10^{-2}T-9.1837\times10^{-5}T^2+1.4454\times10^{-3}T^3} \tag{2}$$

Assuming the produced water is vapor and the vapor is ideal gas, the partial pressure of water at the channels outlets is defined as:

$$p_{O_2,\,out}^{H_2O} = \frac{d_{O_2,\,out}P}{d_{O_2,\,out}+0.622} \tag{3}$$

The $d_{O_2,\,out}$ is the water ratio contained in the outlets oxygen. This ratio is defined as the ratio of mass of water, $m_{O_2,\,out}^{H_2O}$, and mass of oxygen, $m_{O_2,\,out}$, at the outlets.

$$d_{O_2,\,out} = \frac{m_{O_2,\,out}^{H_2O}}{m_{O_2,\,out}} = \frac{m_{prod}^{H_2O}+m_{O_2,\,in}^{H_2O}}{m_{O_2,\,out}} \tag{4}$$

If the water transport in the membrane due to the electro-osmotic drag and diffusion is ignored, the produced water $m_{prod}^{H_2O}$ can be expressed as follow [26]:

$$m_{prod}^{H_2O} = 9.34\times10^{-8}\frac{P_e}{V_C} \tag{5}$$

It is different from the study [26] that the cathode gas flow is pure oxygen other than air, so the oxygen at the outlets is quantified as:

$$m_{O_2,\,out} = 8.29\times10^{-8}(\lambda-1)\frac{P_e}{V_C} \tag{6}$$

where P_e is the electrical output power (W), V_c the mean voltage of each cell in a fuel cell stack (V) and λ is the oxygen stoichiometric ratio.

In our study, the pure oxygen was used without humidification, so the water in the inlet oxygen can be ignored:

$$m_{O_2,\,in}^{H_2O} = 0 \tag{7}$$

The combination of Eqs. (1)–(7) can be solved analytically. Fig. 14 shows the results of the relationship between the temperature (°C) and oxygen stoichiometric ratio (λ) when the oxygen flow is not humidified. If the fuel cells operate at the conditions that the temperature and stoichiometric ratio is under the critical line, the water vapor in cathode channels would condense and the cathode would be flooded.

The curve in Fig. 14 predicts that if the fuel cells operate at 25 °C, the oxygen stoichiometric ratio need to be 31.68 to avoid water condensate. So in our study, when the oxygen flow rate was supplied at 300 ml min^{-1} (stoichiometric ratio 42.9), the membrane intended to be dehydrated. It is important to note that the oxygen flow rate that the curve predicts is higher than the experimental result at low temperature, because the water diffusion from cathode to anode is not calculated. There is much liquid water at low temperature in cathode channels, so some water may transport from cathode to anode due to the concentration difference of the water. But the effect of diffusion can be ignored at high temperature, e.g. at 75 °C, an oxygen stoichiometric ratio of more than 3.98 (the experimental result is 4.29) has to be supplied to avoid liquid water, these theoretical results are consistent with experimental observations.

3.4. Effect of operation time

It has been observed that the water generation continues under operating conditions regardless of temperature or oxygen flow rate during fuel cells operation time. This finding is based on the observation of water condensation in the flow channels. Figs. 15–20 show the condensation evolution of liquid water in the different transparent PEMFCs cathode flow channels, and the change of cell voltage during all the operating time. During this progression, fuel cells were loaded at a constant current of 2 A, a constant temperature of 25 °C, atmospheric pressure conditions and constant oxygen flow rate of 60 ml min^{-1}. Photo (a) was taken while the reactant was supplied but the fuel cells operated at an open circuit mode. The condensation of water could not be observed and

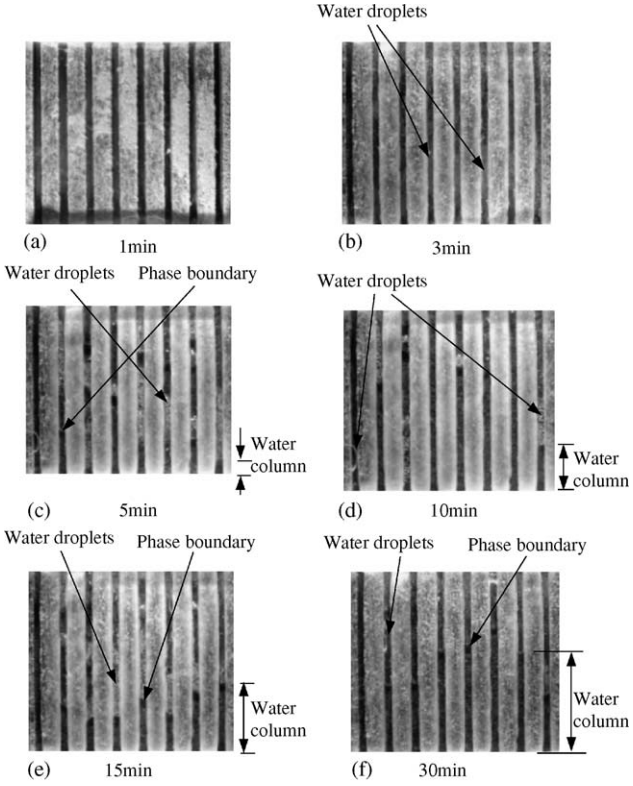

Fig. 15. Effect of operation time on cathode water build-up in parallel channels.

the flow channels were water free. Photos (b–f) were taken after the fuel cells were loaded at a constant current of 2A. The images of liquid water in the parallel channels were recorded at 1 min, 3 min, 5 min, 10 min, 15 min and 30 min, respectively (Figs. 15 and 16). But the images of liquid water in the interdigitated channels and cascade channels were recorded at 1 min, 3 min, 5 min, 15 min, 30 min and 45 min, respectively (Figs. 17–20). Because the flow fields were different, the liquid water appeared and the photos were taken at different times.

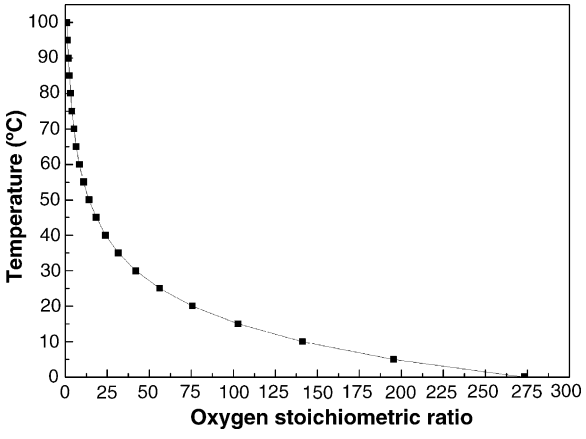

Fig. 14. The oxygen stoichiometric ratio supplied to avoid condensation.

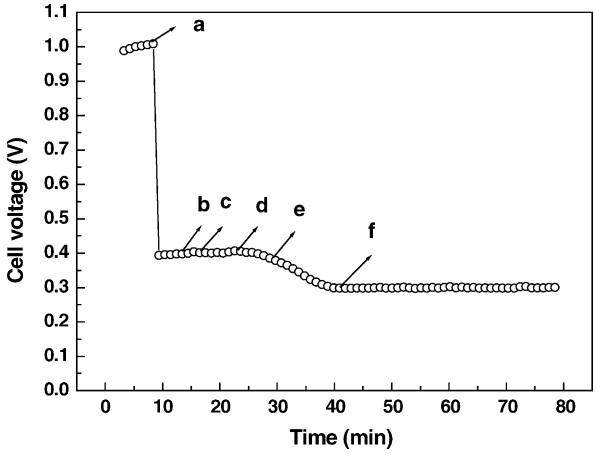

Fig. 16. The cell performance with parallel channels during operation.

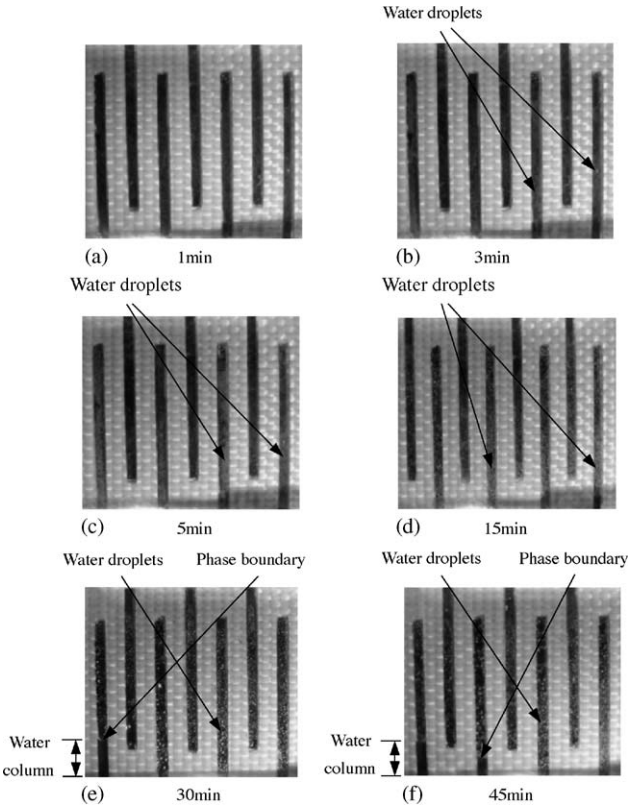

Fig. 17. Effect of operation time on cathode water build-up in interdigitated channels.

The photos imply that the water was penetrating through the gas diffusion layer and reached the flow channels, so the water was appearing on the inner surface of the plexiglass. At the beginning, the current was not loaded, so no water was produced. But after 3 min operation at a constant current of 2 A, fog was visible. It can be seen that the fog consisted of very small water droplets condensed on the inner surface of the plexiglass. Between 5 min and 15 min of operation, with the fuel cells operating, the water droplets increased in size and accumulated in the flow channels. Finally, water columns

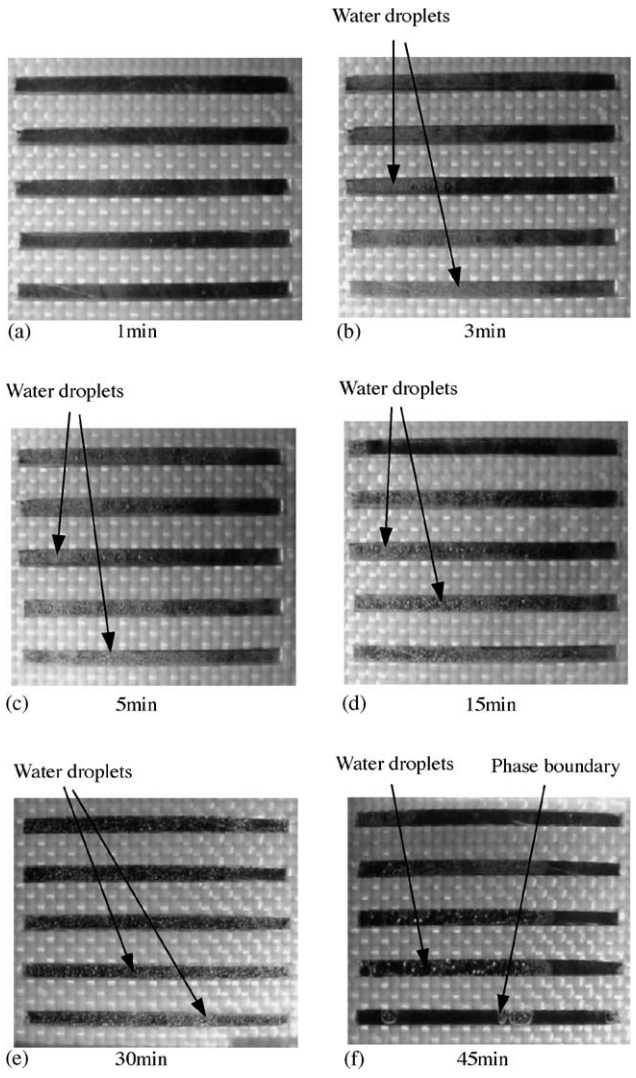

Fig. 19. Effect of operation time on cathode water build-up in cascade channels.

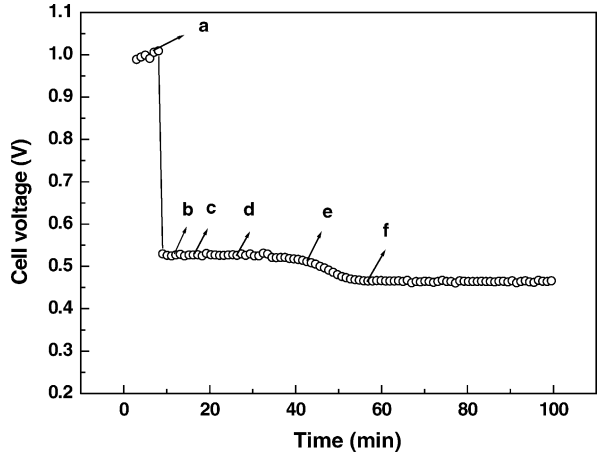

Fig. 18. The cell performance with interdigitated channels during operation.

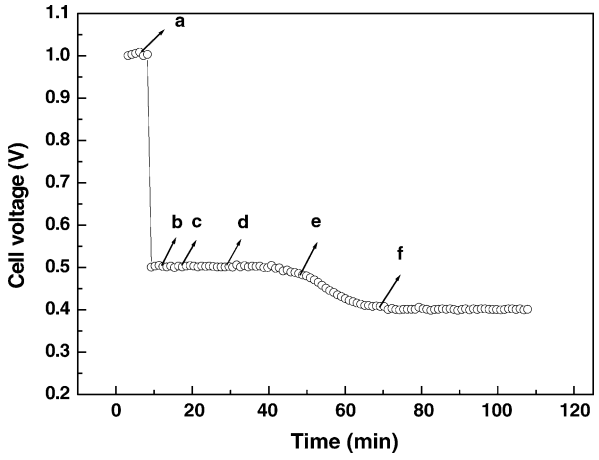

Fig. 20. The cell performance with cascade channels during operation.

appeared in the flow channels. As the result, more and more of the channel volumes were occupied by the liquid water condensate during fuel cells operating.

Fig. 16 shows that the cell performance of the transparent fuel cell with parallel channels dropped gradually while the water droplets increased in size before 15 min of operation. And after 15 min operation, an obvious cell performance drop can be observed. Photo (d) displays the flooding appeared at this time because the liquid water columns were visible in the flow channels. This result is same as the result of Lu et al. [25] in a DMFC, but they did not observe the water columns which filled the flow channels. And in Tübe et al. [26] study, the cell performance decreased gradually before a complete blockage of the channel by water, but an enormous decline (collapse) of cell performance can be observed when the produced water clogged the flow channel. They attributed this enormous decline (collapse) to the water blockage. We found that even with the water columns blockage, no such sudden decline occurred, instead the decline occurred gradually. After 30 min of operation, the fuel cell operated at a new balanced condition but the cell performance was lower than that before the flooding appeared. Under the new balanced condition, electrochemical reaction can only take place in the reduced areas without flooding.

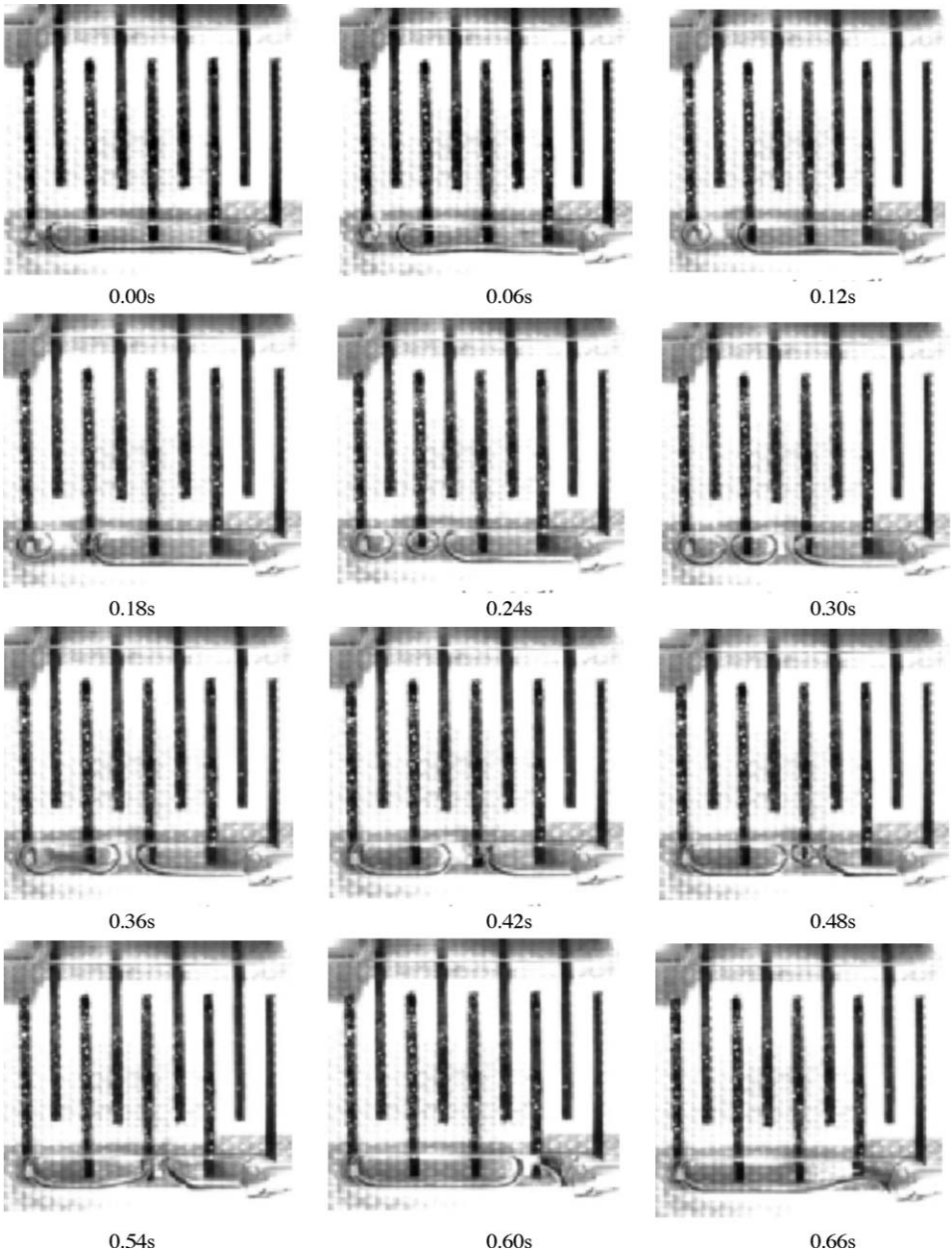

Fig. 21. The water removal out of the manifold of interdigitated flow field.

Figs. 17–20 show that the obvious cell performance drop of the transparent fuel cells with interdigitated channels or cascade channels can be observed after 30 min operation. Because interdigitated channels and cascade channels can enhance mass transfer, the water columns and flooding formed later than in parallel channels. The flooding in interdigitated channels and cascade channels was not serious because the water columns were much smaller than those in parallel channels. Therefore, the cell performances of fuel cells with interdigitated channels or cascade channels are better than those with parallel channels.

The fuel cell performance must decrease at the new balanced condition after the water columns appear. The cell voltages of fuel cells with different flow fields and the decreasing rates were shown in Table 1. The decreasing rates were different because the flooding areas were different. The performance of the fuel cell with parallel flow field after the water flooding was 27.0% lower than that before the water flooding. The decreasing rate with interdigitated flow field was 12.7%, and with cascade flow field was 15.6%. The results indicated that the water flooding made the great impact on cell per-

Table 1
Voltage before and after flooding of different flow fields

	Voltage before flooding (V)	Voltage after flooding (V)	Decreasing rate (%)
Parallel flow field	0.396	0.289	27.0
Interdigitated flow field	0.519	0.453	12.7
Cascade flow field	0.493	0.416	15.6

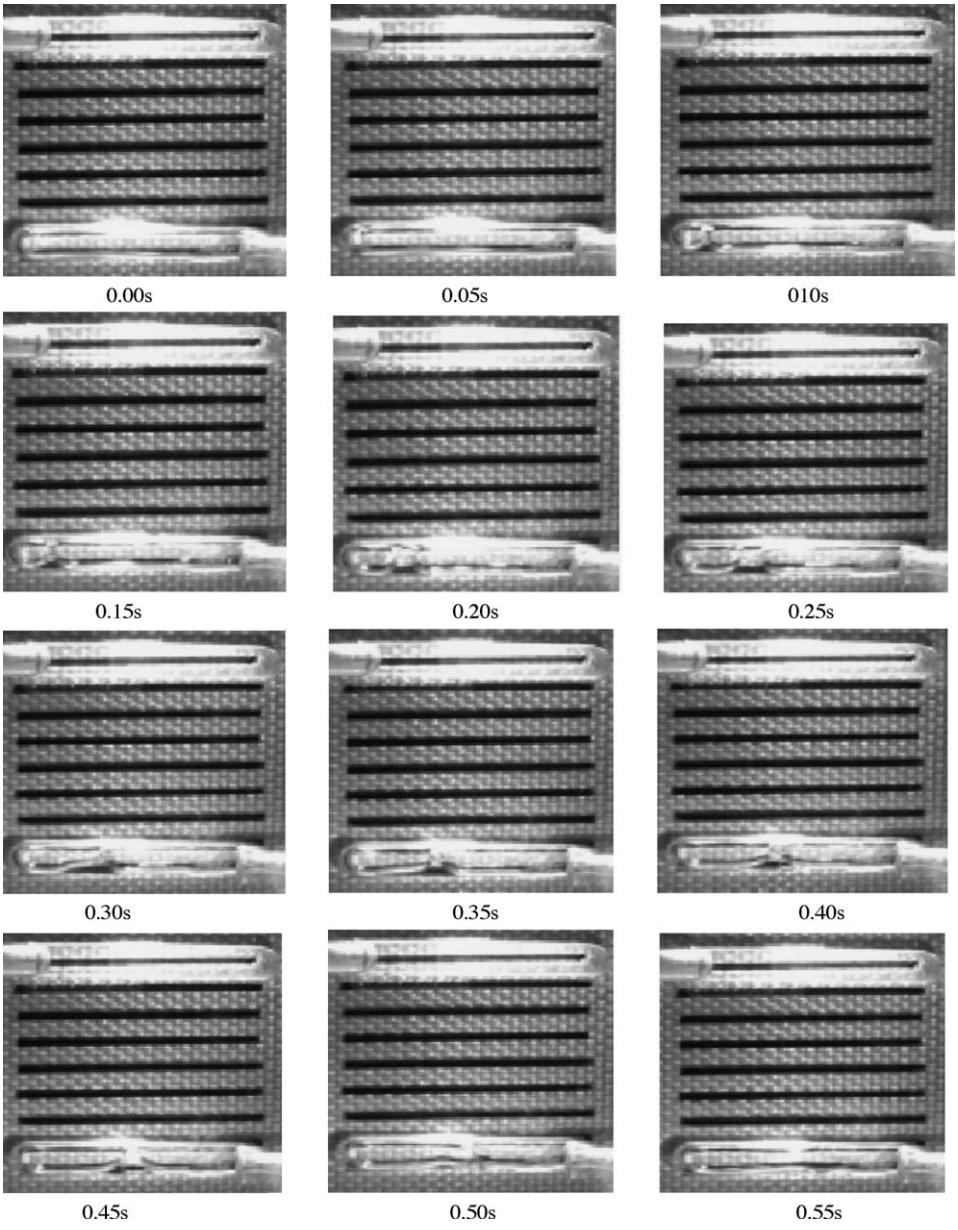

Fig. 22. The water removal out of the manifold of cascade flow field.

formance, because the liquid water made the mass transfer limited. The voltage drop of the fuel cells with cascade flow field or interdigetated flow field was less than the fuel cell with parallel flow field because the water staying in the channels of interdigitated flow field and cascade flow field was less than that in the parallel flow field channels.

3.5. Water removal

The evolution of liquid water removal out of the interdigitated channels and cascade channels was recorded by high-speed video (Figs. 21 and 22). In the interdigitated field, a lot of liquid water was removed out of the channels by the oxygen but stayed in the manifold (main channels). The water accumulated in the manifold (main channels) and was removed by the oxygen. The bubbles were the cathode oxygen that did not react and was discharged from the channels. Because the water column stayed in the manifold (main channels) as a slug, the bubbles formed at the end of the out-flow channels. With the growth of the bubble, the water column was pushed towards the outlet. When the water column moved, other bubbles were formed, joined and increased in size. In the end, all the bubbles amalgamated with each other and became one big bubble, which pushed the water column out of the manifold (main channels). It was the same in the cascade field where the oxygen bubble pushed the water column out of the manifold (main channels).

4. Conclusions

(1) The images of water droplets and flooding in cathode flow channels were recorded by digital camera and high-speed video. Water vapor condensed and accumulated in the cathode channels. Water flooding may occur if the produced water is not removed out of channels in time. This can lead to mass transfer limitation because the condensation of the liquid water stays in the channels and occupies the path of the gas to the reaction sites. The cell performance dropped gradually while the water droplets increased in size, and an obvious cell performance drop can be observed after the water columns appeared.

(2) The condensation of liquid water in the flow channels at high temperature is much less than that at low temperature. At low temperature, there is a lot of liquid water in the flow channels. The liquid water hinders mass transfer. But at very high temperature, there is not enough water to humidify the membrane. Excessive low or high temperatures can lead to deterioration of fuel cells performance.

(3) The cathode gas flow rate can contribute to water removal. Increasing cathode flow rate can remove water out of the cathode flow channels and lead to good cell performance. In this study, the reactant was not humidified. When the stoichiometric ratio of oxygen reached 42.9, the fuel cell performance decreased dramatically because the membrane became too dry, and its conductivity to proton ions reduced.

(4) The interdigitated flow field and cascade flow field can enhance mass transfer when the gas flow is forced to pass through the gas diffusion layer to reach the reaction sites. The water flooding areas in the interdigitated flow channels and cascade flow channels are smaller than that in the parallel flow channels. During the cell operation, the water flooding appears in the interdigitated channels and cascade channels later than appears in parallel channels.

(5) The evolution of water removal out of the manifold (main channel) showed that the bubble flow took place in the manifold (main channel) of interdigitated flow fields and cascade flow fields. The water column stayed in the manifold (main channel) and the oxygen discharged from the flow channels formed the bubbles in the manifold (main channel). The liquid water was pushed out of channels by the cathode gas flow.

This study is helpful for optimizing operation conditions and flow field design to avoid flooding in PEMFCs.

Acknowledgements

The authors would like to acknowledge the following supports of this research: National Natural Science Foundation of China (Grant Nos.: 50236010, 50406010, 50028605), Sino-German Center for Research Promotion of DFG and NSFC (Grant No.: GZ207(101/7)) and Scientific Research Foundation for Doctors of Beijing University of Technology (52005014200401). The authors are grateful to Prof. Guodong Xia, Mr. Maohai Wang and Jielin Jia for the kindly help and discussion and to Peter King P. Eng. for the proof reading and editing.

References

[1] J. Tatiana, P. Freire, E.R. Gonzalez, J. Electroanal. Chem. 503 (2001) 57–68.
[2] V. Mehta, J.S. Cooper, J. Power Sources 114 (2003) 32–53.
[3] S.G. Chalk, J.A. Milliken, J.F. Miller, J. Power Sources 71 (1998) 26–35.
[4] K.H. Choi, D.H. Peck, C.S. Kim, D.R. Shin, T.H. Lee, J. Power Sources 86 (2000) 197–201.
[5] I. Bar-On, R. Kirchain, R. Roth, J. Power Sources 109 (2002) 71–75.
[6] H. Guo, C.F. Ma, M.H. Wang, J. Yu, X. Liu, F. Ye, C.Y. Wang, in: R. Shah (Ed.), Proceedings of First International Conference on Fuel Cell Science, Engineering and Technology, ASME, Rochester, NY, April 21–23, 2003, pp. 471–476.
[7] S.K. Chang, Y.K. Di, H.K. Lee, Y.G. Shul, T.H. Lee, J. Power Sources 108 (2002) 185–191.
[8] L. You, H. Liu, Int. J. Heat Mass Trans. 45 (2002) 2277–2287.
[9] J.J. Baschuk, X. Li, J. Power Sources 86 (2000) 181–196.
[10] D. Picot, R. Metkemeijer, J.J. Bezian, L. Rouveyre, J. Power Sources 75 (1998) 251–260.

[11] S. Miachon, P. Aldebert, J. Power Sources 56 (1995) 31–36.
[12] T.V. Nguyen, R.E. White, J. Electrochem. Soc. 140 (1993) 2178–2186.
[13] T.E. Springer, M.S. Wilson, S. Gottesfeld, J. Electrochem. Soc. 114 (1993) 3513–3526.
[14] J.S. Yi, T.V. Nguyen, J. Electrochem. Soc. 144 (1993) 1149–1159.
[15] T.E. Springer, T.A. Zawodzinski, S. Gottesfeld, J. Electrochem. Soc. 138 (1991) 2334–2342.
[16] T.A. Zawodzinski, C. Derouin, S. Radzinski, R.J. Sherman, V.T. Smith, T.E. Springer, S. Gottesfeld, J. Electrochem. Soc. 140 (1993) 1041–1047.
[17] U. Pasaogullari, C.Y. Wang, J. Electrochem. Soc. 151 (2004) A399–A406.
[18] D.R. Sena, E.A. Ticianelli, V.A. Paganin, E.R. Gonzalez, J. Electroanal. Chem. 477 (2) (1999) 164–170.
[19] F.N. Buchi, S. Srinivasan, J. Electrochem. Soc. 144 (1997) 2767–2772.
[20] I. Wood, L. David, J.S. Yi, T.V. Nguyen, Electrochim. Acta 43 (1998) 3795–3809.
[21] T.H. Yang, Y.G. Yoon, C.S. Kim, S.H. Kwak, K.H. Yoon, J. Power Sources 106 (2002) 328–332.
[22] H.H. Voss, D.P. Wilkinson, P.G. Pickup, M.C. Johnson, B. Vasura, Electrochim. Acta 40 (1995) 321–328.
[23] S.H. Kwaka, T.H. Yang, C.S. Kimb, K.H. Yoona, J. Power Sources 118 (2003) 200–204.
[24] P. Dimitrova, K.A. Friedrich, B. Vogt, U. Stimming, J. Electroanal. Chem. 532 (2002) 75–83.
[25] G.Q. Lu, C.Y. Wang, J. Power Sources 134 (2004) 33–40.
[26] K. Tübe, D. Pócza, C. Hebling, J. Power Sources 124 (2003) 403–414.
[27] A. Hakenjos, H. Muenter, U. Wittstadt, C. Hebling, J. Power Sources 131 (2004) 213–216.
[28] Z. Qi, A. Kaufman, J. Power Sources 111 (2002) 181–184.
[29] Z. Qi, A. Kaufman, J. Power Sources 114 (2003) 21–31.